Modeling vacancies in graphite via the Hückel method

Mattias Hjort and Sven Stafström
Department of Physics and Measurement Technology, IFM, Linköping University, S-581 83 Linköping, Sweden
(Received 21 September 1999)

It is known that when irradiating a graphite surface with ions the predominant source of defects are vacancies. Vacancies are also formed in a growing graphite sheet and cannot be filled. The theoretical work that has been carried out so far on the properties of these defects has only involved quite small model systems. Calculations on graphite, or closely related carbon phases like nanotubes, with randomly distributed vacancies require very large systems allowing only the simplest model to be used. We have used the Hückel method to model vacancies, both ordinary and hydrogenated, by fitting the Hückel energy levels to those resulting from a valence effective Hamiltonian calculation. The three atoms neighboring a vacancy are treated as pseudo-π orbitals and our calculations suggest that they together contribute with one extra π electron to the system. Using this model optical and electronic properties of a graphite sheet as a function of vacancy density have been calculated.

I. INTRODUCTION

Irradiation damage in graphite has been studied very extensively because of its application as a moderator in thermal nuclear reactors.[1] However, theoretical work on the properties of point defects and their effects on the electronic properties of graphite have not been carried out until quite recently. Upon radiating graphite with ion clusters, interstitial atoms between the surface and underlying planes are formed in significant numbers but vacancies are the predominant source of defects.[2]

Density-functional theory has been used on systems with about 50–90 atoms to deduce the electronic structure of a graphite surface containing a few vacancies.[2,3] A tight-binding scheme based on an effective carbon potential has also been used to simulate the migration of vacancies in systems with up to 240 atoms.[4] For systems comprising thousands of atoms one is left with the simple Hückel model (extended Hückel is also possible but will enlarge the size of the problem with at least one order of magnitude). Such a large number of atoms is also common in calculations on closely related structures like nanotubes. A simple scheme to simulate a vacancy by setting the hopping parameters to zero and the on-site energy at the defect site equal to a large value outside the range of the unperturbed density of states has been used both on graphite[5] and on nanotubes.[6] This oversimplification will misplace the highest-occupied molecular orbital–lowest unoccupied molecular orbital (HOMO-LUMO) gap of systems with finite size.

The vacancy itself has been studied by Coulson and others[7–9] treating the defect and its immediate three neighbors as a molecule contained within the graphite matrix. Based on cluster calculations using a self-consistent all-valence linear combination of atomic orbital (LCAO) scheme it has been argued that unlike vacancies in diamond and silicon, many-electron effects are probably very small for the neutral vacancy in graphite and one can safely adopt the one-electron LCAO description.[10]

In this paper we present Hückel parameters for an ordinary vacancy as well as a hydrogenated vacancy. The latter case is interesting since infrared spectroscopy indicates that protonated carbon, in this case, is almost entirely sp^3 coordinated[11] indicating that two hydrogen atoms are bonded to each carbon atom at the vacancy. Naturally this leads to a different electronic structure compared to the ordinary vacancy. Arguments have been made that graphite with this kind of defect will have the properties (especially the optical gap) of hydrogenated amorphous ''diamondlike'' carbon.[12]

II. METHODOLOGY

The Hückel hopping parameter in an all planar π-electron system is assumed to vary with interatomic distance R_{ij} as

$$\beta = \beta_0 e^{\zeta(R_{ij}-R_0)}, \tag{1}$$

where β_0 is the hopping for distance R_0 between the atoms. Together with the on-site energy α, these parameters could be obtained from (least-square) fitting Hückel energy levels of a suitable model system to valence effective Hamiltonian (VEH) levels of the same system, just as in Ref. 13. VEH is an effective potential method that has proven to be versatile in describing valence electronic structures of hydrocarbons with the same type of accuracy as double-zeta *ab initio* self-consistent-field calculations [reproducing valence orbital energies within a mean error of less than 0.001 a.u (Ref. 14)]. VEH results have shown to fit very well to experimental data (ultraviolet photoemission spectroscopy and optical absorption) of π-conjugated systems. In contrast to Hartree-Fock calculations, single particle band gaps and excited states are accurately predicted from VEH calculations.[15] This is the main motive for using the VEH spectrum as a reference.

As a model system to optimize the Hückel parameters for graphite we used an all-benzenoid polycyclic aromatic hydrocarbon[16] (PAH) consisting of 114 carbon atoms. PAH's are planar and can formally be regarded as two-dimensional graphite sections. The all-benzenoid PAH's (constructed by fusing six-membered carbon rings) have the greatest chemical stability and the lowest reactivity of all PAH's and their density-of-states (DOS) curves all resemble

TABLE I. The optimum Hückel parameters obtained from the VEH fit. The three carbon atoms neighboring a vacancy are labeled *A* atoms, while the non-neighboring atoms are labeled *B* atoms (see Fig. 1).

B-atom on-site energy	$\alpha = -6.022$ eV
A-atom (ordinary) on-site energy	$\alpha' = -6.793$ eV
A-atom (hydrogenated) on-site energy	$\alpha'' = -14.365$ eV
B-B hopping	$\beta = \beta_0 e^{\zeta(R_{ij}-R_0)}$
	$\beta_0 = -3.292$ eV
	$\zeta = -1.902$ Å^{-1}
	$R_0 = 1.40$ Å
A-B hopping (ordinary vacancy)	$\beta'_{AB} = -3.37$ eV
A-B hopping (hydrogenated vacancy)	$\beta''_{AB} = -2.34$ eV

that of a graphite layer even for clusters with only a few rings.[17] The C_{114} was geometry optimized using the semiempirical method AM1.[18] In principle such a cluster is too small to obtain the correct vacancy geometry since the effect of the boundary is rather large. We have compared the results within an ensemble of geometry optimizations using different number of vacancies and different vacancy positions to draw conclusions about the relaxed geometry. For the same reason it is also very hard to compare, e.g., the charge distribution from first-priciple methods with the one resulting from our Hückel calculation. Due to relaxation of the cluster boundary slightly different bond lengths were obtained in the cluster making it possible to determine the β_0 and ζ parameters. These parameters were found by fitting 20 Hückel energy levels around the HOMO-LUMO gap to the responding VEH levels. The on-site energies were chosen so that the energy scale coincides with the VEH energies (see Table I). With the interatomic distance of 1.42 Å in graphite these parameters will give a hopping, $\beta = -3.17$ eV, which can be compared to values of the Slonezewski-Weiss-McClure (SWC) model parameter[19] γ_0 found from fitting the single layer tight-binding band structure to *ab initio* bands as well as to experiments. Our hopping is somewhat lower in energy than the *ab initio* value, $\gamma_0 = -2.92$ eV,[22] but is close to the value determined from experiments, $\gamma_0 = -3.16$ eV.[23]

A. The ordinary vacancy

By treating the three carbon atoms surrounding the vacant site (here denoted *A* sites, see Fig. 1) as pseudo-π-orbitals, with Hückel parameters differing from those of the non-neighboring atoms (denoted *B* sites), a fit was done to the VEH spectrum on C_{114} containing two vacancies. The hopping between the three *A* sites should be small (comparable to next-nearest-neighbor interaction) and was set to zero in our model. Since the parameters obtained from fittings on systems with different separation between the vacancies differed negligibly, the parametrization would be valid for various vacancy concentrations. A good fit could however only be obtained if *one extra Hückel energy level is assumed to be occupied in the ground state*. This rather surprising result

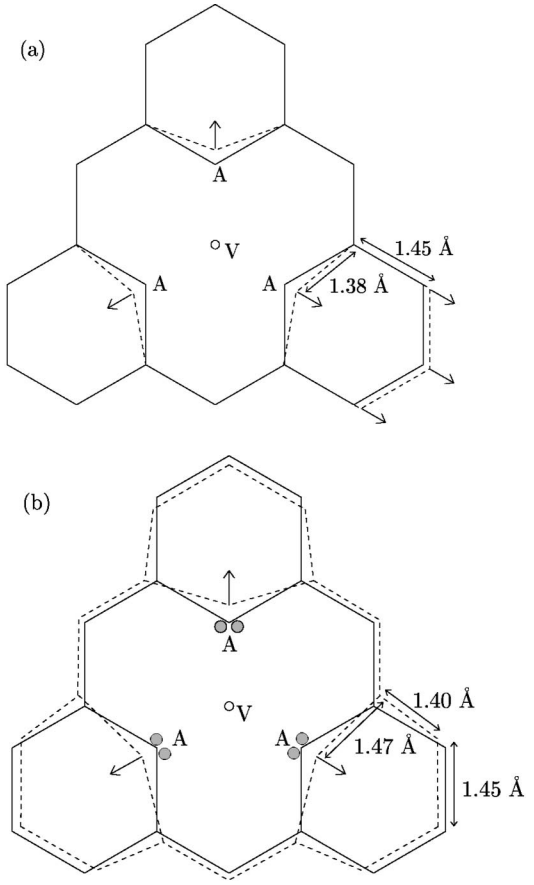

FIG. 1. Schematic picture of the lattice relaxation for the two types of vacancies, ordinary (a) and hydrogenated (b). The relaxation is exaggerated for clarity and the relaxed structure is represented by the dashed lines.

implies that the three *A* atoms together contribute with four π electrons to the system, contradicting the so-called *defect molecule* approach of Coulson *et al.*[8] where the vacancy is represented by the three σ-type sp^2 dangling orbitals that used to bond to the removed atom. Linear combinations of these three orbitals will in that case form pure σ states with no overlap with the π system, while other orbitals on the three *A* atoms are considered to be unaltered.

Consistent with the nonvacancy fit, the geometry of the model system was optimized using the AM1 method allowing the lattice to relax around the vacancies. Our calculation suggests that the relaxation is entirely in plane, which is supported by atomic force microscopy measurements.[24] The *A* sites are displaced symmetrically from the center of the vacancy [see Fig. 1(a)] rendering a bond length of 1.38 Å between *A* and neighboring *B* sites. As indicated in the figure the other atoms surrounding the vacancy are displaced so that one of the bonds involving the next-nearest neighbors is prolonged to 1.45 Å. Other interatomic distances are altered by less than 1%. For simplicity we have only considered the shortening of the *A-B* distance in our Hückel calculations, and the corresponding *A-B* hopping is then $\beta'_{AB} = -3.37$ eV (see Table I).

The optimized on-site energy α' for the *A* atoms corresponds to a lowering of the on-site Coulomb energy. The *A* sites are more attractive than the *B* sites, which is clearly

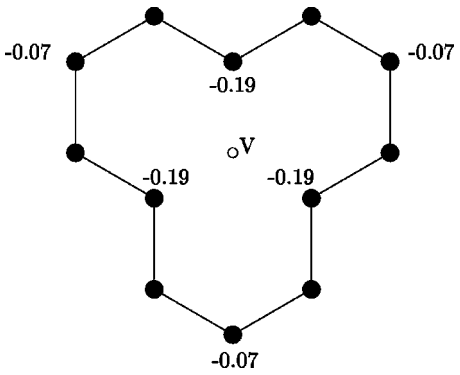

FIG. 2. The additional π charge in units of $|q_e|$ on the atoms surrounding a vacancy (ordinary) obtained from a Hückel calculation.

seen as a π-charge accumulation on the *A* atoms. Our Hückel calculation shows that it is mainly a few states near the Fermi level (E_F) that contribute this extra charge. This is why a vacancy is viewed as a bright spot (protrusion) in scanning tunneling microscopy (STM), since protrusions originate from an increased partial charge density near E_F (which can be seen in the DOS plotted in Fig. 3), although the actual topography is almost flat.[24] We find this additional π charge only on the atoms surrounding the vacancy (see Fig. 2), with $-0.19|q_e|$ on the *A* atoms, nothing on the atoms next to the *A* atoms, and $-0.07|q_e|$ on their second next neighbors as indicated in Fig. 2. Such a charge distribution has qualitatively been predicted by Soto[25] for the ground state of the vacancy. In total about 80% of the extra π electron introduced in our model is localized in the absolute vicinity of the vacancy, a result that supports the assumption that it is the *A* atoms of the defect that contribute this extra π electron.

The localization of the new electronic states introduced by the vacancies has been studied using the inverse participation ratio (IPR), defined as

$$\mathcal{R}_i = \frac{\sum_j c_{ij}^4}{\left(\sum_j c_{ij}^2\right)^2} \tag{2}$$

with c_{ij} being the coefficients in the LCAO expansion of the ith molecular orbital resulting from the Hückel calculations:

$$\Psi_i = \sum_j c_{ij}\phi_j . \tag{3}$$

Hence for normalized states in an infinite system, $\mathcal{R}_i$ ranges from 0 (completely delocalized) to 1 (highly localized). It is clear from the results presented in Sec. III that the new states introduced by the vacancies are fairly localized and from inspection of the wave functions, it was seen that the localization is around the vacancies. This finding agrees very well with the results of electron spin resonance (ESR) measurements, which show that electrons with unpaired spin are localized to this kind of defect.[26] These electrons can be identified within our model as the extra π electrons originating from the *A* atoms.

The optical absorption can be derived by calculating the oscillator strength for transitions between occupied and unoccupied states. The oscillator strength between state Ψ_m and Ψ_n is defined as

$$f_{m\to n} = (E_n - E_m)\mathbf{M}_{m\to n}^2 . \tag{4}$$

The transition moment $\mathbf{M}_{m\to n}$ is calculated from the LCAO coefficients using the following approximative relation:[27]

$$\mathbf{M}_{m\to n} = \sqrt{2}\sum_j c_{mj}c_{nj}\mathbf{r}_j , \tag{5}$$

where $\mathbf{r}_j$ is the vector defining the position of atom j in the coordinate system fixed for the molecule.

B. The hydrogenated vacancy

When graphite is exposed to hydrogen ordinary vacancies present in the graphite can be hydrogenated. Our AM1 calculations show that a hydrogenated vacancy is 6.11 eV lower in energy than the ordinary vacancy plus three isolated hydrogen molecules. As mentioned in Sec. I, the *A* atoms are in this case sp^3 hybridized, i.e., two hydrogen atoms directed out of the plane (one up, one down) bond to each *A* atom. Despite the sp^3 hybridization these carbon atoms together with the attached hydrogen atoms have to be treated as part of the π system since there will be an overlap interaction between the out-of-plane σ-like C-H bonds and the π system.

Hückel parameter values for the hydrogenated vacancy were then obtained in the same way as for the ordinary vacancy, and just as in the former case, one extra Hückel energy level has to be occupied for a fit to be possible.

The Hückel and VEH calculations were performed on systems that were geometry optimized using AM1. Upon relaxation the *A* atoms are displaced in the same way as in the ordinary vacancy. The *A*-*A* distance is, however, enlarged somewhat compared to the previous case because of the hydrogen atoms contained inside the vacancy. This displacement is accompanied by a movement of the surrounding carbon atoms thus prolonging the *A*-*B* bond length to 1.47 Å as shown in Fig. 1. As indicated in this figure more atoms take part in this relaxation compared to the ordinary case but only three different interatomic distances are significantly changed; the *A*-*B* bond length and two other bond lengths in the vicinity of the vacancy are altered by 0.02 Å and 0.03 Å, respectively, and other interatomic distances are changed by less than 1%.

Only the change in *A*-*B* distance has been accounted for in our Hückel calculations. With the optimized parameters the *A*-*B* hopping is $\beta''_{AB} = -2.34$ eV (see Table I) which is 30% lower than for the ordinary vacancy. The *A* atom with hydrogen atoms, all together treated as a pseudo-π orbital, thus has a smaller overlap with the π system. The on-site energy α'' is more than doubled. Note, however, that the site in this case consists of a CH_2 group, which explains the large difference as compared to the previous case. Because of the low α'', states associated with the *A* sites will appear at an energy close to that of α''. These new states are also present in the VEH calculations and correspond to states with a large π content at the *A* atoms.

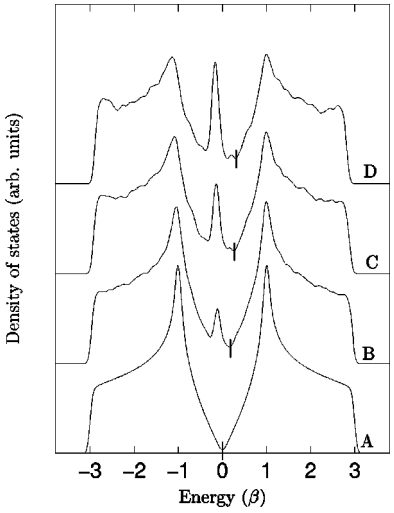

FIG. 3. The Hückel density of states for a graphite sheet with 3786 atoms, plotted for various concentrations of ordinary vacancies with the curves vertically displaced. The Fermi energy is marked in the curves with a vertical bar. (a) No vacancies, (b) 3% vacancies, (c) 6% vacancies, and (d) 8% vacancies.

III. RESULTS

The density of states and the optical absorption of graphite with varying vacancy concentration have been studied for both types of vacancies. We define the vacancy concentration as the number of vacancies divided with the number of carbon atoms in the system with no defects present. The maximum concentration is then about 10% for a random distribution of isolated vacancies.

By performing the calculations on all-benzenoid PAH's of increasing size, conclusions about the infinite system could be made. The number of atoms used in the Hückel calculations were 546, 1986, and 3786, with little difference in the results indicating that the largest system is a good model for the infinite graphite sheet. In Fig. 3 the DOS for the 3786 system is plotted for different vacancy concentrations. The energy scale used is the absolute value of the hopping $\beta(=3.17$ eV) between the carbon atoms in graphite As can be seen, the vacancies create new states that are rather uniform in energy, demonstrating little interaction between the vacancies even for high concentrations. The rise in the IPR values (see Fig. 4) at the vacancy-induced DOS peak shows that these states are much more localized than the states within the graphite bands. By inspection of the wave functions, we can confirm that the states are associated with individual vacancies, in very nice agreement with the STM image of vacancies as ''bright spots.''[24]

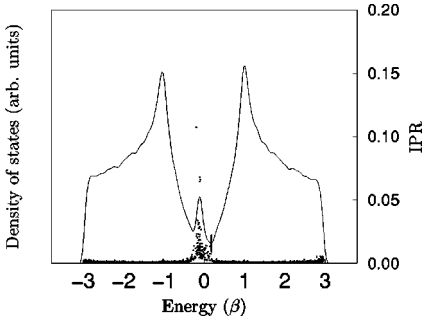

FIG. 4. The Hückel DOS (solid line) and IPR (dots) for a graphite sheet of 3786 atoms with 3% concentration of ordinary vacancies. The Fermi energy is marked in the curve with a vertical bar.

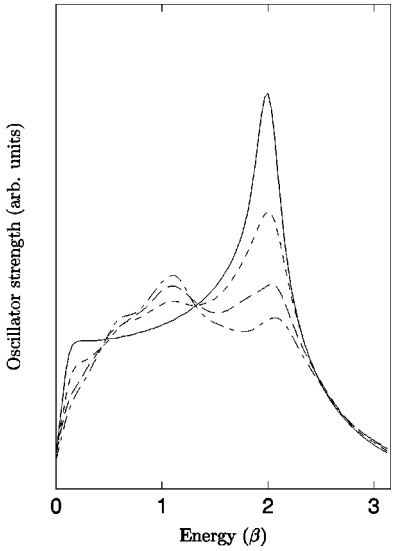

FIG. 5. The oscillator strength for the ordinary vacancies plotted for 0% (—), 3% (- -), 6% (– –) and 8% (- – -) vacancy concentrations.

The oscillator strength for the largest system [shown in Fig. 5(a)] exhibits an absorption peak for the undisturbed graphite at 2β ($=6.34$ eV here). This absorption is clearly due to transitions between the two peaks in the DOS (Fig. 3) and has been found experimentally at about 5 eV.[28] The discrepancy between our calculated value and the experimental data can be explained by the fact that electronic bands from VEH calculations usually are a factor of 1.2–1.3 broader than the measured bandwidth.[15] Since we have used the VEH spectra to obtain Hückel parameters, this effect also shows up in our results. For increasing vacancy concentration, the 2β absorption peak is gradually decreased in intensity and the oscillator strength shifted to a new peak around 1β. Note that the oscillator strength spectrum is quite sensitive to the defect concentration. The 2β peak is reduced by 30% for a defect concentration of 3%.

Reflectivity measurements on neutron-irradiated graphite[28] show that a small absorption band grows around 3 eV while the 5-eV peak diminishes with increasing neutron flux. This is in excellent agreement with our result if again some energy broadening is accounted for. Thus our relatively simple model gives a clear indication of the electronic properties of the vacancy.

It is interesting to note that the Fermi energy (E_F), here taken as the energy in the middle of the HOMO-LUMO ''gap,'' (the ''gap'' is in this case some 0.01 eV only) seems to be located at a local minimum in the DOS spectrum. By comparing Figs. 3 and 5 it is seen that the observed absorption reflects transitions between the vacancy induced states and the states at an energy of 1β. Despite an increase in the DOS at and around E_F, the low-energy absorption actually decreases with higher vacancy concentrations. This is attributed to the strong localization of the vacancy-induced states, which thereby couple more weakly to the delocalized states above E_F.

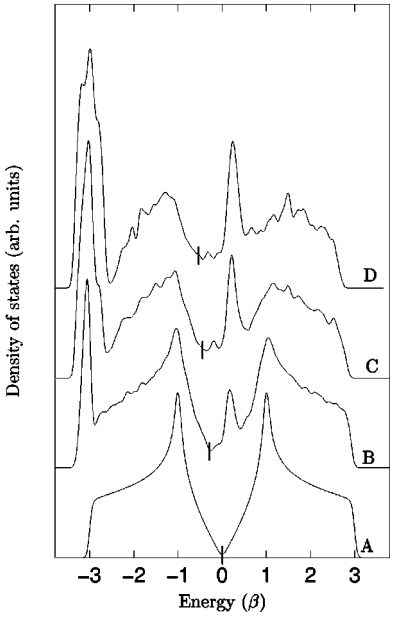

FIG. 6. The Hückel density of states for a graphite sheet with 3786 atoms, plotted for various concentrations of hydrogenated vacancies with the curves vertically displaced. The Fermi energy is marked in the curves with a vertical bar. (a) No vacancies, (b) 3% vacancies, (c) 6% vacancies, and (d) 8% vacancies.

The hydrogenated vacancy has a greater effect on the electronic structure than the ordinary vacancy as seen in Fig. 6. The DOS is considerably modified when the vacancy concentration is increased. Apart from a large peak at low energies (-3β) which is attributed to the low on-site energy of the A atoms, new states also form a peak in the unoccupied region. The number of -1β and 1β states are reduced on account of these new states, leading to a strong suppression of the 5-eV absorption peak when the vacancies are introduced. Transitions between the -1β states and the vacancy-induced states that form the major peak to the right of E_F result in an absorption peak that is slightly blueshifted with increasing vacancy concentration. It is hard to distinguish an optical gap in the data presented in Fig. 7, a quantity that lies in the 0.8–2.0 eV range for hydrogenated amorphous carbon (a-C:H).[12] The presence of such a gap in graphite with hydrogenated vacancies is the key assumption in the defected graphite model for a-C:H proposed by Tamor and Wu.[12] In contrast to this assumption, our results show that the description of the electronic structure in terms of a π system always results in a nonzero oscillator strength at low energies in disagreement with the detection of an optical gap. Other models,[29] assuming large graphite clusters in a-C:H to produce an optical gap of the right size, should also be questioned since our calculations show that such clusters only in special cases (e.g., all benzenoid structures) produce a large gap. More relevant, we believe, is the result of Wang and Ho,[30] that the bonding and antibonding π states of pairs and quartets of sp^2-hybridized atoms embedded in an sp^3-hybridized matrix yield a band gap of about 2 eV. Their calculations refer to diamondlike amorphous carbon, but are likely a good description of a-C:H as well.

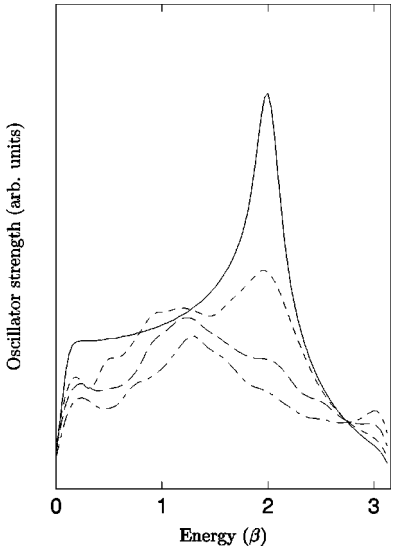

FIG. 7. The oscillator strength for the hydrogenated vacancies plotted for 0% (—), 3% (- -), 6% (– –), and 8% (– – -) vacancy concentrations.

IV. CONCLUSIONS

We have shown that the complicated structure of the electronic wave functions surrounding vacancies in graphite can be accounted for using the simple Hückel method. Our calculations are in agreement with experiments reported for the single ordinary vacancy. Thus the parameter optimization scheme used, involving VEH calculations, seems reliable and the results obtained for the hydrogenated vacancy could be trusted. We emphasize the importance of the extra π electrons induced to the system when vacancies are introduced. For noninteracting vacancies, this extra electron gives rise to an unpaired spin associated with the vacancy, in agreement with ESR data. Local probes of the DOS, like STM, have detected a bright spot associated with the vacancy. We have explained this observation as a result of a strong increase in the DOS just below the Fermi energy in the case of the ordinary vacancy. Finally, we have argued that large graphite clusters in general never give rise to a band gap. Carbon systems with band gaps are therefore better described as sp^3 hybridized.

ACKNOWLEDGMENTS

Financial support from the Swedish Research Council for Engineering Science (TFR) and the Swedish Natural Science Research Council (NFR) is gratefully acknowledged.

[1] B. T. Kelly, *Physics of Graphite* (Applied Science, London, 1981).
[2] K. Nordlund, J. Keinonen, and T. Mattila, Phys. Rev. Lett. **77**, 699 (1996).
[3] N. Takeuchi, J. Valenzuela-Benavides, and L. Morales de la Garza, Surf. Sci. **380**, 190 (1997).
[4] C.H. Xu, C.L. Fu, and D.F. Pedraza, Phys. Rev. B **48**, 13 273 (1993).
[5] K.F. Kelly and N.J. Halas, Surf. Sci. **416**, 1085 (1998).
[6] L. Chico, L.X. Benedict, S.G. Louie, and M.L. Cohen, Phys. Rev. B **54**, 2600 (1996)
[7] C.A. Coulson and M.J. Kearsley, Proc. R. Soc. London, Ser. A **241**, 433 (1957).
[8] C.A. Coulson, M.A. Herraez, M. Leal, E. Santos, and S. Senent, Proc. R. Soc. London, Ser. A **274**, 461 (1963).
[9] A.P.P. Nicholson and D.J. Bacon, Carbon **13**, 275 (1975).
[10] A. Zunger and R. Englman, Phys. Rev. B **17**, 642 (1978).
[11] M.A. Tamor, C.H. Wu, R.O. Carter III, and N.E. Lindsay, Appl. Phys. Lett. **55**, 1388 (1989).
[12] M.A. Tamor and C.H. Wu, J. Appl. Phys. **67**, 1007 (1990).
[13] M. Hjort and S. Stafström, Europhys. Lett. **46**, 382 (1999).
[14] J.-M. André, L.A. Burke, J. Delhalle, G. Nicolas, and P. Durand, Int. J. Quantum Chem., Symp. **13**, 283 (1979), and references therein.
[15] J.-M. André, J. Delhalle, and J.-L. Brédas, *Quantum Chemistry Aided Design of Organic Polymers* (World Scientific, Singapore, 1991).
[16] M. Müller, C. Kübel, and K. Müllen, Chem.-Eur. J. **4**, 2099 (1998).
[17] J. Robertson, Adv. Phys. **35**, 317 (1986).
[18] M.J.S. Dewar, E.G. Zoebisch, E.F. Healy, and J.J.P. Stewart, J. Am. Chem. Soc. **107**, 3902 (1985).
[19] The Slonczewski-Weiss-McClure (SWC) model (Refs. 20 and 21) is a frequently used parametrization of the π bands of graphite near E_F, which is based on the tight-binding method. The quantity γ_0 is just the resonance integral between nearest neighbors.
[20] J.W. McClure, Phys. Rev. **108**, 612 (1957).
[21] J.C. Sloczewski and P.R. Weiss, Phys. Rev. **109**, 272 (1958).
[22] R.C. Tatar and S. Rabii, Phys. Rev. B **25**, 4126 (1982)
[23] E. Mendez, A. Misu, and M.S. Dresselhaus, Phys. Rev. B **21**, 827 (1980).
[24] J.R. Hahn, H. Kang, S. Song, and I.C. Jeon, Phys. Rev. B **53**, R1725 (1996).
[25] M.R. Soto, J. Microsc. **152**, 779 (1988).
[26] T. Tsuzuku and S. Yugo, J. Phys. Soc. Jpn. **24**, 210 (1968).
[27] H. Suzuki, *Electronic Absorption Spectra and Geometry of Organic Molecules* (Academic Press, New York, 1967).
[28] H. Fukutani, A. Yamada, K. Yagi, S. Ooe, K. Higashiyama, H. Kato, T. Iwata, J. Phys. Soc. Jpn. **59**, 3089 (1990).
[29] J. Robertson and E.P. O'Reilly, Phys. Rev. B **35**, 2946 (1987).
[30] C.Z. Wang and K.M. Ho, J. Phys.: Condens. Matter **6**, 239 (1994).